JOURNAL
OF THE AMERICAN CHEMICAL SOCIETY

VOLUME 93, NUMBER 8 APRIL 21, 1971

Physical and Inorganic Chemistry

Theoretical Investigations of the Chemistry of Singlet and Triplet Species. I. Insertion and Abstraction Reactions[1]

R. F. W. Bader* and R. A. Gangi

Contribution from the Department of Chemistry, McMaster University, Hamilton, Ontario, Canada. *Received June 20, 1970*

Abstract: The differing tendencies of singlet and triplet species toward insertion and abstraction are investigated in an SCF calculation of the potential energy surfaces for the model system of $O(^3P,^1D) + H_2(^1\Sigma_g^+)$ to yield either $H_2O(^1A_1)$ on insertion or $OH(^2\Pi) + H(^2S)$ on abstraction. The differences in chemistry of $O(^3P)$ and $O(^1D)$ are related to a polarization of the electronic spins in the substrate bond induced by the approach of the triplet oxygen. Investigation of the spatial distribution of the unpaired spins during the course of the reaction reveals two principal mechanisms of spin polarization, an *unpairing mechanism* corresponding to the localization of charge density with identical spin components on both centers of the substrate bond to yield an unstable triplet insertion product and an *uncoupling mechanism* corresponding to a separate localization of the α and β spin distributions on both centers of the substrate bond to yield the abstraction products. The concept of a spin polarization is found to be a useful one in the interpretation of the chemistry of systems with unpaired spins.

It is well established that the chemistry of a reactant with an open-shell electronic configuration is dependent upon its spin multiplicity. For example, present experimental results indicate that $O(^1D)$,[2-4] $S(^1D)$,[5] and $CH_2(^1A_1)$[6,7] insert directly into C–H bonds of saturated hydrocarbons while $O(^3P)$ and $CH_2(^3\Sigma_g^-)$ undergo only H atom abstraction in these same reactions.[8] The singlet species of these three reactants are found to add to the double bond of an alkene in a stereospecific manner,[9-11] while the addition of triplet oxygen or methylene leads to a mixture of geometrical isomers in the three-membered ring products. For example, the reaction of singlet CH_2 with *cis*- or *trans*-2-butene yields either *cis*- or *trans*-1,2-dimethylcyclopropane, while the triplet form yields a mixture of both products with either reactant.[7] It is the purpose of these investigations to provide both an interpretation of these observations and a theoretical basis for their prediction. The present study is devoted to an investigation of the differing tendencies of the singlet and triplet species toward abstraction and insertion.

The Pauli exclusion principle is of paramount importance in determining the distribution of the unpaired spin density in the triplet system. The basis of the present method is to isolate the additional restrictions imposed by the Pauli principle on the distribution of charge in the triplet system by a calculation and display of the spin density distribution. The distribution of the unpaired spin density accounts for the principle differences in the total molecular charge

(1) This work was reported at the joint meeting of the Chemical Institute of Canada and the American Chemical Society, Toronto, May 22, 1970.
(2) H. Yamazaki and R. J. Cvetanović, *J. Chem. Phys.*, **41**, 3703 (1964).
(3) G. Paraskevonoulos and R. J. Cvetanović, *ibid.*, **50**, 590 (1969).
(4) W. B. DeMore and O. F. Raper, *ibid.*, **46**, 2500 (1967).
(5) A. R. Knight, P. O. Strausz, and H. E. Gunning, *J. Amer. Chem. Soc.*, **85**, 2349 (1963).
(6) W. v. E. Doering, R. G. Buttery, R. G. Laughlin, and N. Chandury, *ibid.*, **78**, 3224 (1956).
(7) R. F. W. Bader and J. I. Generosa, *Can. J. Chem.*, **43**, 1631 (1965).
(8) It has also been noted[3] that while the primary process in the reaction of $O(^1D)$ with saturated hydrocarbons is one of insertion, "some" abstraction of hydrogen does occur.
(9) R. J. Cvetanović, *Can. J. Chem.*, **36**, 623 (1958).
(10) K. S. Sidhu, E. M. Lown, O. P. Strausz, and H. E. Gunning, *J. Amer. Chem. Soc.*, **88**, 254 (1966); E. M. Lown, E. L. Dedio, O. P. Strausz, and H. E. Gunning, *ibid.*, **89**, 1056 (1967).
(11) F. A. L. Anet, R. F. W. Bader, and A.-M. Van der Auwera, *ibid.*, **82**, 3217 (1960).

distributions of the singlet and triplet systems, and hence for the observed differences in their chemistry.

The method involves the calculation of the potential energy surfaces for the singlet and triplet systems followed by a calculation of the total charge and spin density distributions. We have applied this method to a study of the insertion and abstraction reactions of $O(^1D,^3P)$ with $H_2(^1\Sigma_g^+)$. The singlet and triplet potential surfaces are found to be strikingly different and from their nature one can conclude that singlet oxygen inserts by choice and abstracts by chance while triplet oxygen abstracts by necessity, conclusions which are in complete accord with experimental findings regarding the relative chemical behavior of singlet and triplet species.

While the surfaces account for the difference in chemistry of the singlet and triplet species in terms of the energetics of the systems, they do not provide an explanation or rationale for the differences. This can be obtained from a knowledge of the spin density distribution. The importance of changes in the distribution of the spin density during the triplet reaction is emphasized when one notes that states of atoms (and diatomic molecules) derived from the same configuration possess nearly identical charge distributions.[12] Thus for large initial separations between the reactants, the charge distributions of the singlet and triplet systems are identical, and the ^1D and ^3P oxygen atoms exert identical coulombic fields on H_2, or the hydrocarbon substrate. Yet, even for relatively large separations, the charge distributions of the singlet and triplet systems begin to diverge significantly corresponding to very different energy paths for the two reactions. It is proposed that the increasing divergence of the distributions of charge density in the singlet and triplet systems be related to a spin polarization induced in the triplet system by the presence of the two unpaired electrons.

In general, one can envisage two principal kinds of spin polarization. In the linear approach of $O(^3P)$ to a substrate AB giving the abstraction reaction

$$O(^3P) + AB \longrightarrow OA + B$$

the presence of unpaired α spin density on oxygen could uncouple the spins of the bonded electron pair in AB, inducing an excess β spin density on the neighboring nucleus A and an excess α spin density on B. Thus the bond in AB is broken by a spin polarization corresponding to separate localizations of excess α and β spin density at the two ends of the bond. A second type of spin polarization could be operative in the "insertion" approach, the approach of the oxygen atom along the bisector of the AB bond axis. In this symmetrical case the AB bond could be weakened by the transfer of the excess spin density from oxygen to both A and B, a process whose net effect is to unpair the spins of the two electrons in the AB bond. The presence of charge density with an identical spin component on both centers of the substrate bond will result in a localization of the total charge density on each nucleus and in a great reduction in charge density in the bond region of AB.

(12) P. E. Cade, R. F. W. Bader, and J. R. Pelletier, *J. Chem. Phys.*, in press.

Both mechanisms, the spin-uncoupling and spin-transfer mechanisms, are found in the reactions of $O(^3P)$ with H_2. Before describing the results of the theoretical investigation a brief discussion of spin densities is presented.

The Spin-Density Distribution

The distribution function for the total electronic charge density $\rho(r)$ is given by

$$\rho(r) = N\int\psi^*(X_1, X_2, \ldots, X_N)\psi(X_1, X_2, \ldots, X_N)\mathrm{d}s_1\ldots\mathrm{d}s_N\mathrm{d}r_2\ldots\mathrm{d}r_N \quad (1)$$

where X_i denotes the space and spin coordinates of the ith electron. The product $\rho(r)\mathrm{d}r$ yields the total amount of electronic charge, irrespective of its spin component, in the volume element $\mathrm{d}r$. Integration of $\rho(r)$ over all space yields the total number of electrons, N.

$$\int\rho(r)\mathrm{d}r = N$$

When the wave function is approximated by a single determinant, eq 1 reduces to

$$\rho(r) = \sum_i n_i\phi_i^*(r)\phi_i(r) \quad (2)$$

where n_i is the occupation number of the ith space orbital ϕ_i. If every space orbital is allowed to be distinct when associated with either an α or a β spin component (denoted by ϕ_j^α or ϕ_k^β, respectively), then the total charge $\rho(r)$ may be equated to separate contributions from the α and the β orbital densities

$$\rho(r) = \sum_j n_j\phi_j^{*\alpha}(r)\phi_j^\alpha(r) + \sum_k n_k\phi_k^{*\beta}(r)\phi_k^\beta(r) = \rho^\alpha(r) + \rho^\beta(r) \quad (3)$$

In restricted Hartree–Fock theory for a closed-shell system the space orbitals from the sets j and k occur in $N/2$ pairs with $\phi_j^\alpha = \phi_k^\beta$ for each pair. In this case $\rho^\alpha(r) = \rho^\beta(r) = {}^1/_2\rho(r)$.

We define the spin density distribution function $\sigma(r)$ as

$$\sigma(r) = \rho^\alpha(r) - \rho^\beta(r) \quad (4)$$

that is, $\sigma(r)\mathrm{d}r$ is the *number* of excess α ($\sigma(r) > 0$) or β ($\sigma(r) < 0$) electrons in the volume element $\mathrm{d}r$. Integration of $\sigma(r)$ over all space yields the total number of unpaired electrons in the system[13]

$$\int\sigma(r)\mathrm{d}r = N^\alpha \text{ or } -N^\beta$$

where N^α and N^β are the number of excess α or β electrons, respectively.

For a closed-shell system $\sigma(r)$ is zero at every point in space. In the restricted Hartree–Fock approximation to an open-shell system, a state with the maximum value of M_s (the z component of the spin angular momentum) gives

$$\sigma(r) = \sum_i^\alpha \phi_i(r)\phi_i(r) - \sum_j^\beta \phi_j(r)\phi_j(r)$$

where the sums run over only the singly occupied orbitals containing the unpaired α or β electrons. In the unrestricted Hartree–Fock approximation, which

(13) We define $\sigma(r)$ as a pure number density. McWeeny [R. McWeeny, *Rev. Mod. Phys.*, 32, 335 (1960)] defines his spin density distribution $Q_s(r)$ in such a way that it integrates to the M_s eigenvalue. The two definitions are related through $\sigma(r) = 2Q_s(r)$. For a discussion of spin densities the reader is referred to R. McWeeny and B. T. Sutcliffe, "Methods of Molecular Quantum Mechanics," Vol. II, Academic Press, New York, N. Y., 1969, p 104.

allows for different spatial orbitals for different spins, all the orbitals are singly occupied and hence all of the orbital densities contribute to $\sigma(r)$ at every point in space. The unrestricted method is the one employed in the present calculations.

The difference between the restricted and unrestricted Hartree–Fock methods is illustrated for the case of the $^2\Pi$ ground state of the hydroxyl radical, a product common to both the singlet and triplet abstraction reactions. The contour map of $\rho(r)$ obtained in an unrestricted calculation and shown in Figure 1 is essentially superimposable on the corresponding map of the restricted Hartree–Fock approximation to the total charge distribution.[14] The two approximations to $\sigma(r)$, however, exhibit small but important differences. In the restricted Hartree–Fock approximation the electronic configuration of the OH radical is $1\sigma^2 2\sigma^2 3\sigma^2 1\pi^3$, *i.e.*, a single unpaired electron in the 1π orbital. In this approximation the spin density distribution would equal the distribution of charge obtained from a single electron in the 1π orbital, which in OH is a $2p\pi$ atomic-like distribution localized on the oxygen, slightly polarized toward the proton.[14] While the map of the unpaired spin density $\sigma(r)$ obtained from the unrestricted calculation and shown in Figure 1 does resemble a $2p\pi$-like charge distribution in its gross features, there are important differences between the two distributions. The nodal line along the internuclear axis is missing; the distribution is more diffuse and more striking; a spin polarization is present within the total charge distribution. Spin density of opposite sign is induced along the bond axis in the region of the proton and in the nonbonded region of the oxygen. Thus there is a relative displacement of the α and β spin distributions assumed to be paired in the restricted Hartree–Fock approximation. Correspondingly, an integration of just the positive spin density contributions to $\sigma(r)$ would yield a number slightly greater than unity indicating that the excess α electron has induced a slight spin polarization within the remaining charge distribution.

The $\sigma(r)$ distribution obtained here and in particular its pattern of spin polarization agrees in detail with the results of Bender and Davidson[15] obtained from extensive configuration-interaction calculations on the diatomic hydrides. The unpaired spin density at the proton in OH($^2\Pi$) has been measured by Radford,[16] who obtains a value of -0.0167 au. Our calculated value using a single configuration-unrestricted Hartree–Fock calculation is -0.0248 au, while Kayama[17] in a CI calculation using ten configurations obtains a value of -0.0152 au.

The SCF Calculations

The details of the present calculations have been reported elsewhere.[18] We summarize here only their most important features and the philosophy underlying the charge-density approach. The present aim is to provide an interpretation of the differences in singlet and triplet chemistry in terms of the molecular charge

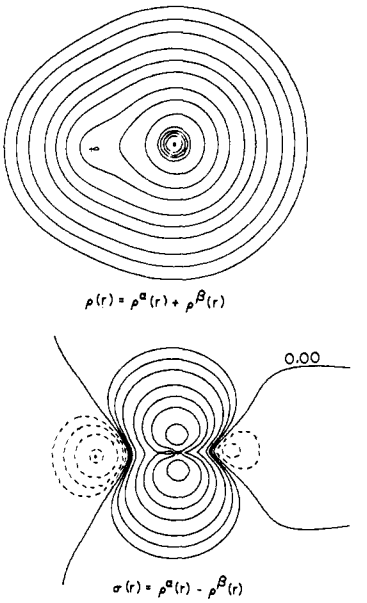

Figure 1. Contour maps of the total charge and spin density distributions for OH($^2\Pi$). The proton is the left-hand nucleus. In *total charge density maps* the contours increase in value from the outermost member, in the order 2×10^{-n}, 4×10^{-n}, 8×10^{-n} au for decreasing values of n beginning with $n = 3$; in *spin density maps* the solid and dashed contours increase (excess α) or decrease (excess β), respectively, from the zero contour in the order $\pm 2 \times 10^{-n}$, $\pm 4 \times 10^{-n}$, $\pm 8 \times 10^{-n}$ au for decreasing values of n beginning with $n = 3$ (1 au of charge density = 6.749 $e^-/Å^3$).

distribution. It is well known that Hartree–Fock wave functions yield excellent approximations to the true molecular charge distributions.[19,20] In fact, the Hartree–Fock charge distribution and one obtained from a much more extended calculation are indistinguishable when portrayed in the form of a contour map such as that employed in the present work.[21] For this reason all of the charge distributions displayed here are obtained from wave functions which are close to the Hartree–Fock limit.

A Hartree–Fock wave function, since it is a product of one-electron functions, does not correlate the motions of electrons with opposite spin, but since it is an antisymmetrized sum of such products, does account for the complete negative correlation of the motions of electrons with the same spin,[13] as required by the Pauli principle. Thus Hartree–Fock energies exhibit a well-defined and physically understandable error, the correlation error.[22] It is because the Hartree–Fock method reflects chemical changes more faithfully in the charge distribution than in the energy that we base the interpretive aspects of this work on the properties of, and changes in the charge distribution.

A study of a reaction does minimize the importance of the correlation error in the energy, since one is concerned with changes in the error rather than with its absolute magnitude; in other words one is not interested in the total error in the energy relative to the separated electrons and nuclei. In particular, for reactions between closed-shell systems yielding closed-shell products (the number of paired electrons remains

(14) R. F. W. Bader, I. Keaveny, and P. E. Cade, *J. Chem. Phys.*, 47, 3381 (1967).
(15) Unpublished results of C. F. Bender and E. R. Davidson.
(16) H. E. Radford, *Phys. Rev.*, 126, 1035 (1962).
(17) K. Kayama, *J. Chem. Phys.*, 39, 1507 (1963).
(18) R. F. W. Bader and R. A. Gangi, *Chem. Phys. Lett.*, 6, 312 (1970).
(19) G. G. Hall, *Phil. Mag.*, 6, 249 (1961).
(20) C. W. Kern and M. Karplus, *J. Chem. Phys.*, 40, 1374 (1964).
(21) R. F. W. Bader and A. K. Chandra, *Can. J. Chem.*, 46, 953 (1968).
(22) P.-O. Löwdin, *Advan. Chem. Phys.*, 2, 207 (1959).

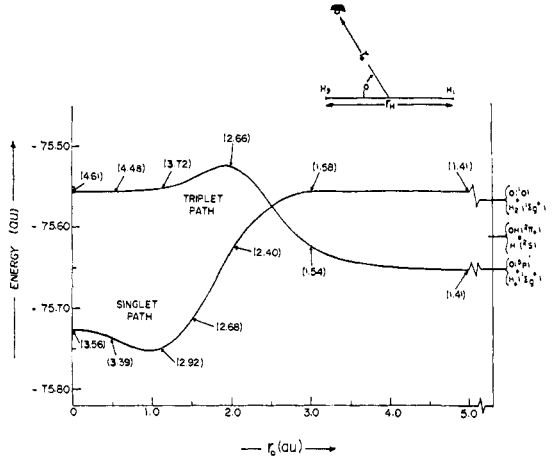

Figure 2. The minimum-energy paths for the singlet and triplet symmetrical insertion reactions as determined by the small basis-set calculations. The bracketed values indicate the H–H internuclear separation. The relative energy of the abstraction products (H + OH) is also indicated. The inset defines the three independent parameters r_O, r_H, and α.

constant), the Hartree–Fock estimates of ΔE are, in general, correct to ±11 kcal/mol.[23] In the present case, because of the open-shell nature of the configuration giving the ^1D and ^3P states of oxygen, the errors in the energy are in general larger than the ±11 kcal/mol quoted above. The origin of the error is, however, understood and the theoretical potential surfaces are to be interpreted bearing in mind the error, its origin, and its change during the reaction. In every case where possible, the experimental value of an energy change is quoted along with its theoretical estimate. In the final section, after the mechanisms of the reactions are understood, a rough scaling of the surfaces with respect to the changes in the correlation error during the course of the reactions is suggested. Fortunately, in the present calculations the positions and heights of the barriers on the energy surfaces which distinguish singlet from triplet chemistry are all of such a magnitude as to be well defined within the errors introduced by the correlation effect.

The energy surfaces were mapped out in SCF calculations using a Gaussian basis set of a size sufficient to give a reliable representation of the major features of the surface. Calculations were then repeated for selected points *along the minimum energy path* as defined by the small basis set using a larger basis set. The small basis set consisted of either 18 or 19 GTO's depending on the surface being calculated. The large set correspondingly used 38 or 39 such functions and included d functions on oxygen and p functions on hydrogen. For details, see ref 18. The large basis set yields charge distributions of near-Hartree–Fock accuracy and energies differing by 0.02 au from this same limit. On both surfaces and at widely different geometries the energy change in going from the small to the large basis set never differs by more than 0.03 au.

Thus the surfaces and geometries of the minimum-energy paths are defined by the small basis-set calculations, and the portrayals of these surfaces (Figures 2 and 5) refer to these calculations. However, the energy values quoted in the text for barriers along the reaction coordinate and for the energies of reaction all refer to the large basis-set calculations, as do all the portrayals of $\rho(r)$ and $\sigma(r)$.

All the surfaces were calculated using the unrestricted Hartree–Fock method.[24] It is possible that serious contamination by states of higher multiplicity may thus occur. The extent of this contamination in the present calculations was monitored by the computation of $\langle S^2 \rangle$ at each point and was found to be unimportant. Except for two points, the values of $\langle S^2 \rangle$ never deviated from 2.0 by more than about 0.01. The two exceptions are the linear triplet on the insertion path and the transition point in the abstraction path which have values of 2.04 and 2.07, respectively.

For the reaction path defined below as the singlet insertion, a limited CI was employed which included, in addition to the ground-state configuration

$$(1a_1)^2(2a_1)^2(1b_2)^2(3a_1)^2(1b_1)^2 \qquad {}^1A_1$$

the following two determinants

$$(1a_1)^2(2a_1)^2(1b_2)^2(3a_1)^2(4a_1)^2 \qquad {}^1A_1$$

$$(1a_1)^2(2a_1)^2(3a_1)^2(1b_1)^2(4a_1)^2 \qquad {}^1A_1$$

These latter determinants were constructed using the virtual orbital $4a_1$ from the ground-state SCF wave function. It was necessary to include all three configurations in order to provide the proper limiting description of $O(^1D)$. The results of the SCF calculation on the ground state were found to be indistinguishable from those of a restricted calculation.

A multideterminantal approach was also necessary in the calculation of the singlet abstraction reaction in order that both reactants and products be correctly defined. The three determinants used were

$$1\sigma\overline{1\sigma}'2\sigma\overline{2\sigma}'3\sigma\overline{3\sigma}'\pi_x\overline{\pi}_x'\overline{\pi}_z4\sigma \qquad \text{A}$$

$$1\sigma\overline{1\sigma}'2\sigma\overline{2\sigma}'3\sigma\overline{3\sigma}'\pi_x\overline{\pi}_x'\pi_z\overline{4\sigma} \qquad \text{B}$$

$$1\sigma\overline{1\sigma}'2\sigma\overline{2\sigma}'\overline{3\sigma}\overline{3\sigma}'\pi_x\overline{\pi}_x'\pi_z4\sigma \qquad \text{C}$$

In the limit O + H_2 the space parts of $\overline{3\sigma}'$ and 4σ become identical and represent the $1\sigma_g^2$ orbital in H_2. Determinant B thus drops out. In the limit OH + H the space parts of $\overline{3\sigma}'$ and 3σ become identical and represent the $3\sigma^2$ orbital in OH. In this case determinant C drops out. For intermediate points all three determinants contribute to the representation. The electronic configurations of the triplets written in restricted notation are

$$(1a_1)^2(2a_1)^2(1b_2)^2(3a_1)^2 1b_1 4a_1 \qquad {}^3B_1$$

$$(1\sigma)^2(2\sigma)^2(3\sigma)^2(1\pi)^3 4\sigma \qquad {}^3\Pi$$

The Insertion Reactions

The potential surfaces of the H_2O system involve three independent internal coordinates which we choose to be r_O, the distance between the oxygen nucleus and the midpoint of the H–H separation; r_H, the H–H separation; and α, the angle between them, as indicated in Figure 2. By keeping α fixed at 90°, and finding the minimum energy as a function of r_H for fixed values of r_O extending from infinity to zero, one obtains a *minimum-energy path* on a surface restricted to a C_{2v} geometry of the reactants (or a $D_{\infty h}$ geometry in the linear case

(23) L. C. Snyder, *J. Chem. Phys.*, **46**, 3602 (1967).

(24) A. W. Salotto and L. Burnelle, *Chem. Phys. Lett.*, **3**, 80 (1969); *J. Chem. Phys.*, **52**, 2936 (1970); **53**, 333 (1970).

of $r_O = 0$). The singlet and triplet reaction paths thus obtained define the following *symmetrical insertion* reactions

$$H_2(^1\Sigma_g^+) + O(^3P) \longrightarrow H_2O(^3\Pi_u) \qquad \Delta E_e = +67 \text{ kcal/mol}$$

$$H_2(^1\Sigma_g^+) + O(^1D) \longrightarrow H_2O(^1A_1) \qquad \Delta E_e = -126 \text{ kcal/mol},$$
$$\Delta E_{exp} = -169 \text{ kcal/mol}$$

The reaction paths are illustrated in Figure 2 plotted as energy *vs.* r_O. The variation in r_H along either minimum-energy path is indicated by the bracketed values shown on the diagram for a number of selected points.

After a slight increase for large values of r_O, the singlet surface shows a continuous decrease in energy leading to a ground state with a minimum of −76.04383 au at an O–H bond length of 1.80784 au and a bond angle of 111° 42′. The corresponding experimental values are 1.80887 au and 104° 31′. The potential barrier separating this configuration of the nuclei from the linear one is 33 kcal/mol with an accompanying increase in r_H from 2.995 to 3.559 au. The curvature of the surface for motion along the coordinate r_H, d^2E/dr_H^2, decreases from a value of 0.399 au for $r_O = \infty$ to 0.088 au at $r_O = 2.0$ au, and increases again to a value of 0.421 at $r_O = 0.0$. The value of d^2E/dr_H^2 at $r_O = \infty$ corresponds favorably with the experimental value 0.368 au, the force constant for H_2. Thus the singlet surface is initially steep for motion at right angles to the minimum energy path indicated in Figure 2, becoming quite flat around $r_O = 2.0$ au, and then steep again for values of $r_O < 2.0$ au.

The triplet state of water has an energy minimum in the linear HOH configuration on the *symmetric* surface. Furthermore, since $d^2E/dr_H^2 > 0$ at all points along the triplet energy path, the linear triplet form of water is stable to any *symmetrical* displacement of the nuclei. The value of d^2E/dr_H^2 decreases rapidly from 0.399 au for large values of r_O to 0.052 au at $r_O = 2.00$ au, and finally reaches a value of 0.040 au in the linear configuration. Not only is the triplet surface flatter than the singlet one for extension of the H–H distance, the values of r_H along the triplet minimum energy path are larger than those for corresponding r_O values on the singlet path.

The symmetrical insertion of triplet oxygen thus forces the hydrogens apart, leading to the formation of a very loosely bound intermediate. The binding of the protons is, in fact, so weak that there is no intermediate form of triplet water stable to all internal motions. For values of $r_O < 3.00$ au, the triplet configurations are all unstable to an *unsymmetrical* motion of the nuclei, the energy exhibiting a continuous decrease as the oxygen is moved off center toward one of the protons with a simultaneous increase in r_H to yield $OH(^2\Pi) + H(^2S)$. The energy minimum on the symmetric triplet path is, therefore, a saddle point and does not represent a stable configuration for triplet water. Miller, *et al.*,[25] have determined a portion of the energy surface for the corresponding singlet excited state of water at a fixed bond angle of 105°. The state is also found to be unstable to an asymmetric dissociation yielding $H(^2S) + OH(^2\Pi)$.

Contour maps of the total charge distributions for selected configurations along the singlet and triplet reaction coordinates are shown in Figure 3. At $r_O = 4.00$ au (not shown in the Figure) the perturbations are quite small and the charge distributions resemble closely those of the isolated reactants.[26] At $r_O = 3.00$ au the effect of the increasing H–H separation is apparent in the pinching of the high-density (0.2 au) contour encircling the protons in both the singlet and triplet systems. For values of $r_O < 3.00$ au the energy of the singlet path decreases while that of the triplet begins a rapid increase. Correspondingly, marked differences appear in the charge distributions of the singlet and triplet systems. After an initial scission of the 0.2-au contour encompassing the protons due to the further increase in r_H in both systems ($r_O = 2.00$ au), the singlet system is characterized by a complete merging of the hydrogen and oxygen charge distributions into a single, compact distribution with contours of high value encompassing and binding all three nuclei. The result ($r_O = 1.11$ au) is the stable, low energy insertion product, $H_2O(^1A_1)$.

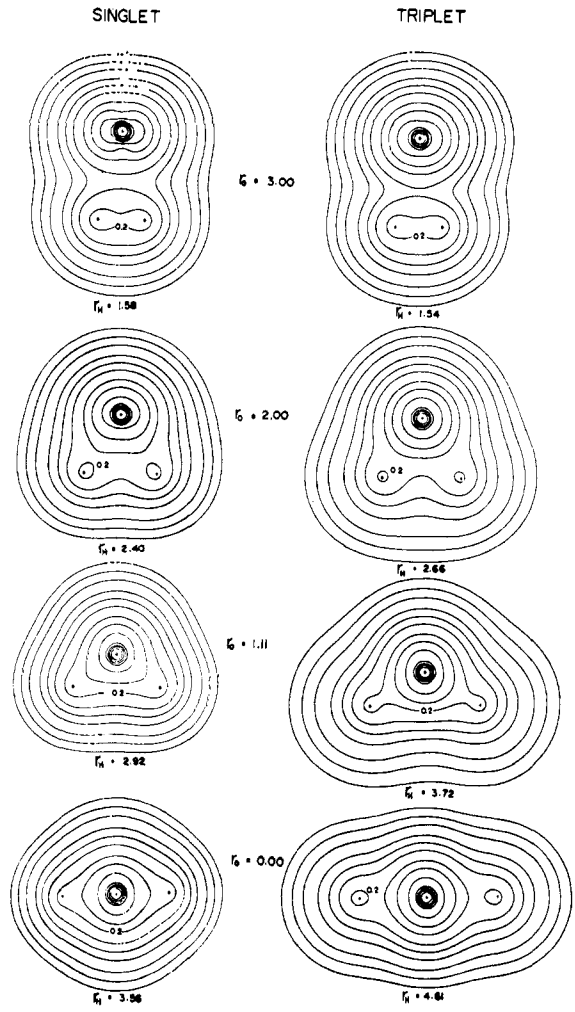

Figure 3. Contour maps of the total charge distributions in the plane of the nuclei for the symmetrical singlet and triplet insertion reactions. (See caption for Figure 1 for contour values.)

(25) K. J. Miller, S. R. Mielczarek, and M. Krauss, *J. Chem. Phys.*, 51, 26 (1969).

(26) The distribution of charge in the region of oxygen is different for the triplet and singlet cases even for large values of r_O, since different components of the ^3P and ^1D states of oxygen are mixed to describe the initial stages of the reaction. Spherical averages of the ^1D and ^3P charge distributions on oxygen are nearly identical, as stated earlier. The pinched effect of the 0.4-au contour encircling the oxygen nucleus in the singlet case (at $r_O \geq 3.0$ au) is characteristic of cases in which there is an excess of π to σ electrons in the region of oxygen; the $A^1\Sigma^+$ state of LiO^+, for example, which dissociates into $O(^1D)$ and $Li^+(^1S)$: unpublished results of P. E. Cade and R. F. W. Bader.

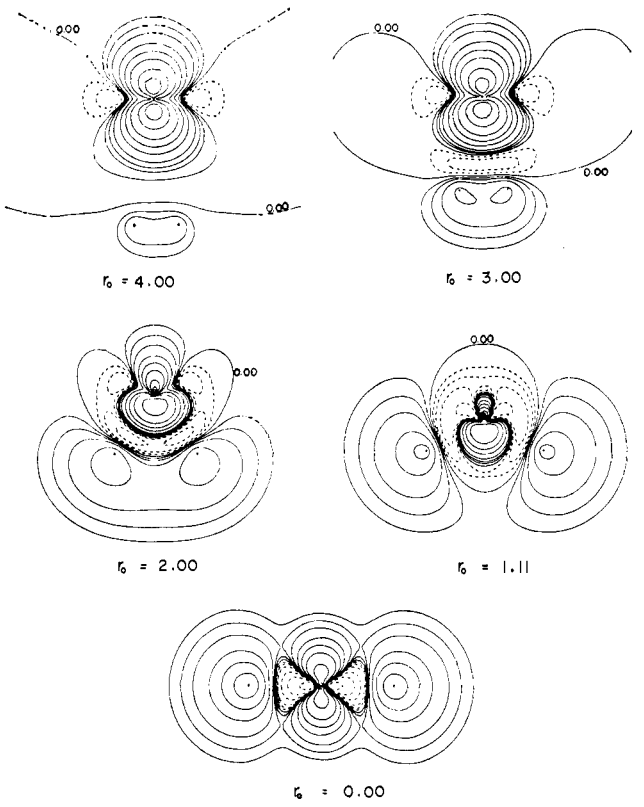

Figure 4. Contour maps of the spin density distributions for the symmetrical triplet insertion reaction. Positive or excess-α spin density is denoted by solid contours, negative or excess-β spin density by dashed contours. (See caption for Figure 1 for contour values.)

In the triplet system further motion along the minimum energy path leads to a marked expansion of the charge density into the nonbonded regions of the protons ($r_O \leqslant 2.00$ au). This expansion results in a very diffuse distribution in the regions of the protons and in low concentrations of charge density between each pair of nuclei. These effects are maximized at $r_O = 0.00$ au and in addition there is a *separate localization* of the charge density in the region of each nucleus. In contrast, even when the singlet system is forced into the linear geometry at a cost of ~33 kcal/mol, the charge distribution is still compact with all three nuclei encompassed by contours up to ~0.3 au in value.

We now attempt to account for the gross differences in the charge distributions of the singlet and triplet systems and hence for their different reaction coordinates in terms of the spatial distribution of spin density $\sigma(r)$. Spin density distributions in the plane of the nuclei for configurations along the minimum energy triplet path are illustrated in Figure 4. The contour maps of $\sigma(r)$ are for the $M_s = 1$ spin component of the triplet state, that is, with two unpaired α electrons which initially are localized on the oxygen atom. One of the unpaired spins remains almost entirely localized in a distribution which has its maximum values in a plane perpendicular to the plane of the nuclei shown in the diagram.

Even at $r_O = 4.00$ au a spin polarization is evident in the system, corresponding to the creation of excess α spin density in the charge distribution of the hydrogen molecule. Simultaneous with this, is the appearance of excess β spin density in the region of the oxygen. Both of these effects are enhanced as r_O is decreased, with the excess α spin population forming diffuse, expanded distributions of increasing extent in the regions of the protons. A comparison of the contour values in the $\rho(r)$ and $\sigma(r)$ distributions for $r_O = 2.00$ au and 1.11 au indicates that almost 100% of the outermost nonbonded charge density on the protons represented by the 0.002-, 0.004-, and 0.008-au contours in the $\rho(r)$ maps is composed of α spin density. The separation, localization, and enhancement of positive spin density increases until, in the linear configuration, the α spin density accounts for 80–100% of the total charge density in the spatial region of each proton. Although the integral of $\sigma(r)$ over all space will yield two electrons (or spins), the appearance of negative spin density in the $\sigma(r)$ distribution indicates that charge density previously paired has been unpaired. That is, integration of just the positive contours of $\sigma(r)$ over all space will yield more than two electrons.

The behavior of the spin density distribution along the reaction coordinate does account for the major differences in the charge distributions and chemistry of the singlet and triplet species. At $r_O = 2.00$ and 1.11 au the extreme localization of charge density with an identical spin component on each proton results in a great reduction in the total charge density in the region between the protons. This follows as a consequence of the requirements of the Pauli principle on the two-electron charge density[13] that

$$\rho^{\alpha\,\alpha}(r_1,r_2) \rightarrow 0$$

for $r_1 \rightarrow r_2$. The spin polarization very effectively weakens the bond in the hydrogen molecule. In effect *the spin polarization caused by the approach of $O(^3P)$ corresponds to a quasi-excitation of H_2 from its singlet ground state to its unbound $^3\Sigma_u^+$ state*, a state characterized by a localization of charge density on each nucleus, each distribution being polarized away from the other into its nonbonded region.

The two localized, almost pure α spin distributions on each proton are most widely separated and the energy minimized in the linear configuration. Thus the mechanism of triplet insertion corresponds to an inducement of identical spin distributions on each center of the substrate bond, an effect which weakens the bond and leads to the formation of a loosely bound metastable intermediate.

The nonstereospecific addition of $O(^3P)$ to an alkene double bond may also be accounted for in terms of this same mechanism of transfer of triplet character from oxygen to the substrate bond. In this case the approach of triplet oxygen could induce an unpairing of the spins of the two electrons in the π bond of the alkene. The increasing localization of α spin density on each carbon would correspond to an *adiabatic* conversion of the alkene to a triplet state modified, of course, by the presence of the oxygen. The triplet state of ethylene is known to possess a twisted geometry[27] and hence deexcitation of the triplet adduct to the singlet surface would yield both forms of any possible geometrical isomer.

The Abstraction Reactions

The singlet and triplet abstraction reactions are defined as[28]

(27) J. W. Moskowitz and M. C. Harrison, *J. Chem. Phys.*, 42, 1726 (1965); M. Barfield, *ibid.*, 47, 3831 (1967).

$O(^3P) + H_2(^1\Sigma_g^+) \rightarrow OH(^2\Pi) + H(^2S)$ $\Delta E_e = +17$, $\Delta E_{exp} = +1$ kcal/mol

$O(^1D) + H_2(^1\Sigma_g^+) \rightarrow OH(^2\Pi) + H(^2S)$ $\Delta E_e = -38$, $\Delta E_{exp} = -45$ kcal/mol

Both reactions give identical products, the triplet reaction being endothermic and the singlet reaction very exothermic. The minimum energy paths on these surfaces, when the systems are confined to a linear geometry, are obtained by setting $\alpha = 0°$ and finding the energy minimum as a function of r_H for a series of fixed values of r_O. For values of r_O greater than about 2.7 and 3.1 au in the singlet and triplet cases, respectively, the energy as a function of r_H for a fixed r_O exhibits a double minimum corresponding to the central H being bonded to the end H (H—H + O) or to the O (H + H—O). Contour maps of the singlet and triplet potential surfaces are shown in Figure 5 plotted as functions of r_O and r_H.

The triplet reaction is predicted to have an energy maximum at an intermediate point along the minimum energy path and hence an energy of activation for both forward and reverse reactions. The minimum energy path is parallel to the r_O axis for $r_O > 3.7$ au and thus the H_2 molecule remains tightly bound until the oxygen is relatively close. Between $r_O = 3.7$ and 3.2 au the energy increases rapidly and the H_2 separation is increased to approximately 2.0 au. In this region of maximum energy along the reaction path there is a transfer of the central H followed by a rapid increase in r_H. The maximum, lying 35.2 kcal/mol above the combined energies of the reactants, occurs at $r_O = 3.150$ au with H–H and O–H separations of 2.075 and 2.112 au, respectively.

The energy maximum in the linear singlet reaction lies 24.7 kcal/mol above the combined energy of the reactants. Thus, there is an activation energy for both the forward and reverse reactions just as in the case of the linear triplet. The major difference in the two paths is the much sharper decrease in the energy of the singlet after this maximum has been reached, so that at the limit of $r_O = \infty$, both the singlet and the triplet paths coalesce into the common products $OH(^2\Pi)$ and $H(^2S)$. The geometry of the singlet species at the energy maximum is $r_O = 3.125$ au, with H–H and O–H separations of 1.675 and 2.287 au, respectively. Thus the maximum in the singlet abstraction occurs at a point where the H–H distance is shorter and the O–H distance longer than that of the triplet abstraction.

Both surfaces are relatively flat for motion perpendicular to the reaction coordinate in the region of the energy maximum, particularly in the triplet case. The experimental equilibrium bond length of $OH(^2\Pi)$ is 1.834 au compared to the O–H separations of 2.112 and 2.287 au found for the triplet and singlet transition states, respectively.

The O–H separation in the singlet case should account for approximately 25 of the 63 kcal/mol of energy which the transition state has in excess of the combined energies of the products. Thus a considerable fraction of this excess energy will appear in the form of translational kinetic energy as the two products separate.

(28) The Hartree–Fock estimates of ΔE for the triplet and singlet reactions are +13.7 and −36.7 kcal/mol, respectively.

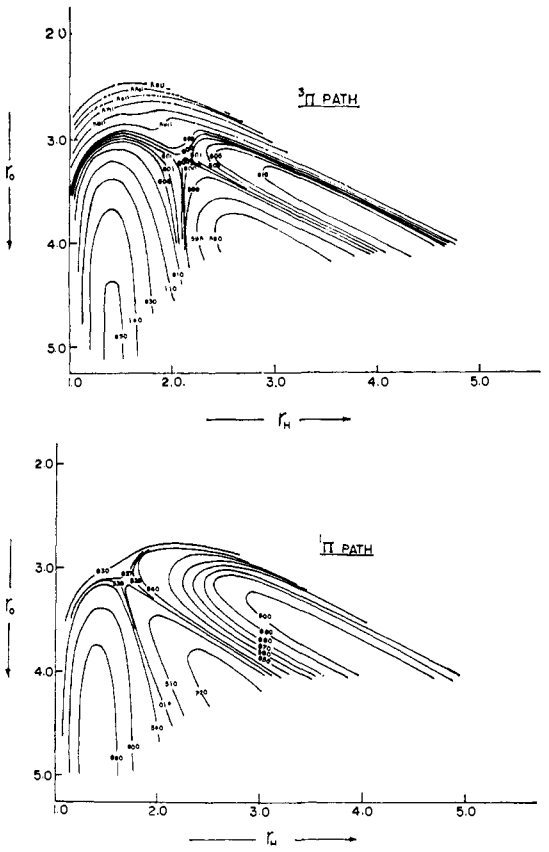

Figure 5. Contour maps of the potential energy surfaces for the linear triplet and singlet abstraction reactions as determined by the small basis-set calculations. A contour of value x denotes an energy in atomic units of $-(75.000 + x)$; *e.g.*, the energy defined by the 650 contour is −75.650 au. The contours increase in steps of 0.010 au except for the region of the transition state where smaller increments are indicated.

Motion of the system from the linear to the symmetric (C_{2v}) surface occurs only when the energy exhibits a continuous decrease for an increase in α from 0 to 90°. At $r_O = 4.0$ au and $r_H = 1.4$ au on the singlet surface, there is a relatively deep flat-bottomed well extending from $\alpha = 30°$ to $\alpha = 60°$. Thus any linear approach of $O(^1D)$ to H_2 has available to it a path of lower energy leading eventually to the insertion path and its potential minimum. (However, see the discussion below regarding the possibility of an "off-angle" abstraction of hydrogen.)

At $r_O = 4.0$ au and $r_H = 1.4$ au on the triplet surface, on the other hand, the energy surface is essentially flat for a variation in α from 0 to 90°. Since the energy of the symmetric path rises very rapidly to values above those of the linear path in the triplet reaction for values of $r_O < 4.0$ au, the minimum-energy path for the reaction of $O(^3P) + H_2$ is the one leading to abstraction. As indicated earlier, the symmetric configurations on the C_{2v} surface are unstable with respect to separation into $OH(^2\Pi) + H(^2S)$ for $r_O < 3.0$ au. In fact all points considered on the triplet surface are connected by downhill paths to either $H_2(^1\Sigma_g^+) + O(^3P)$ or $H(^2S) + OH(^2\Pi)$.

The total charge distributions for the triplet and singlet abstraction reactions are illustrated in Figure 6. The approach of singlet oxygen causes a larger perturbation of the H_2 charge distribution in the initial stages of the reaction and up to the transition state than does

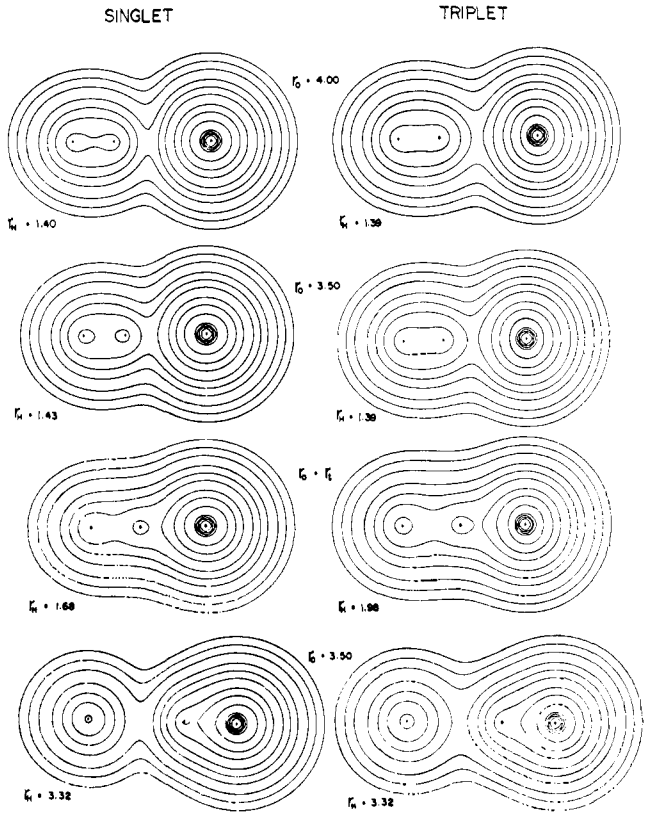

Figure 6. Contour maps of the total charge distributions for the singlet and triplet abstraction reactions. The pair of maps for $r_O = r_t$ are for configurations in the regions of the transition states; the singlet map is for $r_O = 3.125$ au and the triplet one for $r_O = 3.225$ au.

the triplet oxygen. At $r_O = 4.0$ au in the singlet reaction the 0.2-au contour encompassing the protons is severely contracted at the H_2 bond midpoint, and at $r_O = 3.5$ au it is severed, indicating a localization of the charge density on each proton and a removal of charge density from the H–H internuclear region. The next pair of maps is for configurations in the regions of the transition states ($r_O = 3.150$ au for the $^3\Pi$ state and $r_O = 3.125$ au for the $^1\Pi$ state). The triplet configuration shows a separation of the H_2 fragment into an H atom and a proton partially bonded to the oxygen. (In the OH radical the 0.2-au contour encompasses both the proton and the oxygen nucleus, a situation approached very closely in $\rho(r)$ for the $^3\Pi$ transition state.) In the $^1\Pi$ system the charge density in the region of the outermost proton has been considerably decreased.[29] After passage over the energy barrier, the charge distributions of both the singlet and triplet systems acquire the separate features characteristic of the OH($^2\Pi$) and H(^2S) distributions. Thus at $r_O = 3.5$ au the charge distributions correspond to the partial overlap of the charge distributions of a hydrogen atom and an OH radical. (The charge contours in the OH fragment should be compared with the contour map of the molecular charge distribution of OH($^2\Pi$), Figure 1.) At $r_O = 4.0$ au (not shown in Figure 6) the separation into the products is essentially complete.

(29) The $^1\Pi$ state cannot be described in terms of the same single electronic configuration defining the $^3\Pi$ state. Thus the charge distributions of the singlet and triplet states are not expected to be identical even at identical geometries.

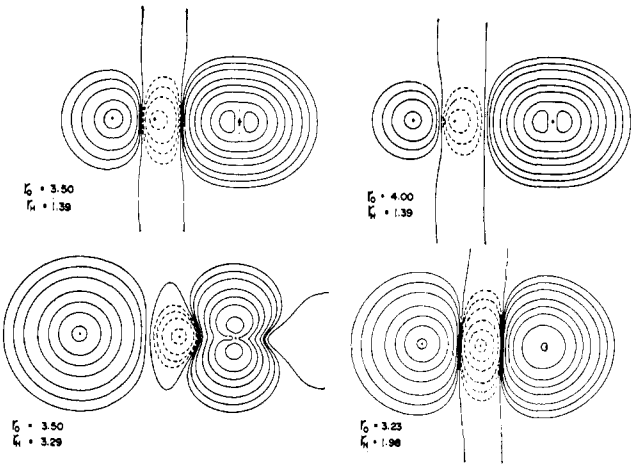

Figure 7. Contour maps of the spin density distributions for the triplet abstraction reaction. The map in the upper right-hand corner ($r_O = 4.00$, $r_H = 1.39$) is for the initial stage of the reaction, that in the lower left-hand corner ($r_O = 3.50$, $r_H = 3.29$) for the separation into the products H + OH.

Figure 7 illustrates the polarization of the spin density distribution during the course of the triplet reaction. The maps are for the $M_s = 1$ component of the triplet state and are axially symmetric.

The spin polarization induced by the approach of triplet oxygen provides an example of the uncoupling mechanism. The α and β spin distributions are perfectly paired in the isolated hydrogen molecule and $\sigma(r)$ is initially everywhere zero. The approach of the triplet oxygen causes an uncoupling of the spin densities in the hydrogen molecule, α spin density migrating to the end proton and β spin density to the adjacent proton. This effect increases as r_O is decreased. The total amount of excess β spin induced on the central proton is always less than the amount of excess α spin induced on the end proton. Thus, in addition to the uncoupling mechanism there is a net migration of α spin density from the oxygen to the end proton and a counter migration of β spin density. In the region of the transition state ($r_O = 3.150$ au) the positive spin density is almost equally partitioned between the oxygen nucleus and the end proton, the partitioning of spin density required for the production of two products, each in a doublet state (*i.e.*, each with one unpaired electron). At the transition state, the distribution of the positive spin density accounts for approximately 90% of the total charge density in the region of the end proton. After passage through the transition state, the spin distribution rapidly acquires the form characteristic of the OH($^2\Pi$) species and of a hydrogen atom (for a hydrogen atom $\rho(r) = \sigma(r)$).

The triplet insertion and abstraction reactions are predicted to have very different activation energies (82 and 35 kcal/mol, respectively) and different mechanisms for their spin polarizations. In the symmetrical insertion reaction the localization of spin density with the same component on both hydrogen atoms forces the protons apart early in the reaction. Thus this type of spin polarization is characterized by a large increase in energy as the substrate bond is stretched, hindering at the same time bond formation with oxygen. Only in the final linear configuration in the insertion approach can the O–H separation be decreased to a value where weak

bonds are formed between the hydrogen nuclei and the inserted oxygen. In the linear abstraction approach, the inducement of spin densities with opposite components on each hydrogen nucleus allows for a bonding of the oxygen with one proton with a minimum breaking of the original H_2 bond. The energy of activation is thus greatly reduced. As the angle α is varied from 90 to 0°, there will be a smooth transition of the spin polarization from the one characteristic of insertion to the one characteristic of abstraction. Correspondingly, the energy will exhibit a continuous decrease as the distribution of spin density is changed to one which allows for an increasing amount of bonding of the oxygen with one of the hydrogen atoms.

The reaction of $O(^1D)$ with H_2 has been studied by DeMore[30] in liquid argon at 87°K and by Paraskevonoulos and Cvetanović[31] in the gas phase. DeMore finds zero energies of activation for the reactions of singlet oxygen with H_2 to yield H_2O and transient OH + H, and with CH_4 to yield CH_3OH and transient CH_3 + OH.[4] These results are consistent with the surfaces presented here for $O(^1D)$ if all of the OH product observed in the reactions derives from the decomposition of the vibrationally excited water or methanol molecules formed in the insertion reaction. Paraskevonoulos and Cvetanović, however, in their studies of the reactions of $O(^1D)$ with isobutane[3] and in particular with neopentane[32] have shown that OH and hydrocarbon radicals are formed at pressures well above those required for stabilization of the corresponding alcohols formed by the insertion reaction. Thus hydrogen atom abstraction does occur, although not necessarily by a linear approach as investigated here. The present results indicate a lower energy approach for large r_O when α lies between the extremes of 0 and 90°. If this effect persists for smaller values of r_O in the off-angle approach it is possible that the radical products could be formed with little or no energy of activation from a complex in which the oxygen is strongly bonded to one hydrogen and only weakly bonded to the other (or to the carbon in the hydrocarbon reaction).[32] Whether one chooses to call this an asymmetrical decomposition of the forming insertion product or a nonlinear abstraction reaction is unimportant. The present results do show that the linear "classical abstraction" reaction has a relatively high energy of activation (~25 kcal/mol) and is probably not an important pathway. However, the nature of the surface with respect to a variation in the angle of approach and the associated possibility of an asymmetrical abstraction should be further investigated.[32]

In agreement with the present calculations, nonzero energies of activation are found for the abstraction of hydrogen from saturated hydrocarbons by triplet oxygen. Heron and Huie[33] find that the activation energy increases with increasing strength of the C–H bond, their maximum measured value of 8.9 kcal/mol being found in the reaction with methane. The value of 35 kcal/mol calculated here for the abstraction of hydrogen from H_2 is undoubtedly too high. Westenberg and de Haas[34] give an experimental value of 10.2 kcal/mol. The correlation error in the OH radical is larger than it is for the reactants H_2 and $O(^3P)$, primarily because the correlation of the unpaired electrons in a triplet state is well accounted for by even a restricted Hartree–Fock wave function. The change in the correlation error between reactants and products is approximately 16 kcal/mol. Since the present analysis shows that the formation of the OH fragment is essentially complete at the transition state in the triplet abstraction reaction, virtually the whole of the correlation error is present at this point. Correcting for this error reduces the approximate estimate of the activation energy to 19 kcal/mol.

The inducement of spin density with an identical spin component on each center of a substrate bond as found here for the $O(^3P)$ insertion reaction should apply for the triplet insertion into a C–H bond of a saturated hydrocarbon as well. Thus the observed lack of insertion products in the triplet reactions with saturated hydrocarbons[2-4] is well accounted for in terms of the high activation barriers and the resulting instability of the triplet insertion adduct associated with this mechanism of spin polarization.

Acknowledgment. We wish to thank Dr. J. W. Moskowitz for providing us with a current version of POLYATOM and Drs. L. Burnelle and A. W. Salotto for a copy of their unrestricted Hartree–Fock program. We also thank Dr. C. F. Bender for a copy of the unpublished spin density distribution for the $CH(^2\Pi)$ radical.

(30) W. B. DeMore, *J. Chem. Phys.*, 47, 2777 (1967).
(31) G. Paraskevonoulos and R. J. Cvetanović, *J. Amer. Chem. Soc.*, 91, 7572 (1969).
(32) G. Paraskevonoulos and R. J. Cvetanović, *J. Chem. Phys.*, 52, 5821 (1970).
(33) J. T. Heron and R. E. Huie, *J. Phys. Chem.*, 73, 3327 (1969).
(34) A. A. Westenberg and N. de Haas, *J. Chem. Phys.*, 50, 2512 (1969).